



# The Effect of Nb<sub>2</sub>O<sub>5</sub>-Ni Coatings on the Microstructural and Corrosion Behavior on Carbon Steel for Marine Application

Rana Afif Anae<sup>1</sup> · Abdullah A. Abdulkarim<sup>2</sup> · Mathew T. Mathew<sup>3</sup> · Hiyam Mezher Jedy<sup>4</sup>

Received: 10 July 2020 / Revised: 21 September 2020 / Accepted: 14 October 2020 / Published online: 23 October 2020  
© Springer Nature Switzerland AG 2020

## Abstract

In this study, we developed Nb<sub>2</sub>O<sub>5</sub>-Ni composite coatings on carbon steel by DC sputtering technique. The effect of Nb<sub>2</sub>O<sub>5</sub> particulate on the Ni coating properties was investigated. The weight percents of Nb<sub>2</sub>O<sub>5</sub> in Ni coating were 0, 12, 15, and 30 wt%. The structural properties of the composite coatings were characterized using scanning electron microscope equipped with energy-dispersive spectrometer. The microhardness and thickness of composite coatings were measured, in addition to examine the corrosion properties in 3.5% NaCl using MLab 200 potentiostat/galvanostat with linear polarization technique. The results showed that hardness value increased to 164 HV for 30 wt% Niobia compared with 155 HV for Ni coating and the thickness increased slightly for Nb<sub>2</sub>O<sub>5</sub>-Ni composite coatings. The corrosion performance improved to obtain efficiencies better than Ni coating alone.

**Keywords** Nb<sub>2</sub>O<sub>5</sub>-Ni coatings · Microstructure · Microhardness · Corrosion behavior

## 1 Introduction

Nickel coating is resistant to dry gases, oil, soaps, and petrol. Nickel coating increases resistance to many corrosion types in different media, but not to nitric acid and environments containing chloride. The life of nickel coatings may be further increased by a thin overlay of microcracked chromium because corrosion would not penetrate the nickel directly, but will spread laterally. Nickel is generally plated as a part of multilayer coating system. The coating system consisting of the dull nickel, bright nickel, and chromium layer is called the composite nickel coating. Nickel coatings are commonly applied to zinc, steel, and other metals to provide protection against corrosion. Incorporating other materials (metals or ceramics) with nickel coating can also be referred to

as composite coating. On the other hand, applying ceramic coatings on metal surfaces gives protection against corrosion and erosion with some disadvantages. In this work, Nb<sub>2</sub>O<sub>5</sub>-Ni composite coatings were investigated. There are many works focused on Nb<sub>2</sub>O<sub>5</sub> coating using different techniques [1–10].

## 2 Experimental Procedures

### 2.1 Materials Preparation and Co-deposition

Structural steel (AISI 1015) with the dimensions of (20 mm × 20 mm × 2 mm) were used as the substrate, its chemical composition (wt%) was as follows: C 0.161, Si 0.271, Mn 0.425, P 0.0073, S 0.0049, and balance of Fe. Before the coating test, the substrate was in turn ground with SiC abrasive papers of 400, 600, 800, and 1000 in water, rinsed with alcohol, dried in the air, and sandblasted with alumina grit.

DC sputtering technique was achieved in a low-pressure gas discharge device consisting of an evacuated chamber, a target (cathode), and anode disk of stainless steel. The cathode was placed opposite the anode and provided the gas discharge of electrical field with 4 KV DC power supply. The cathode electrode insulated with diameter of

✉ Rana Afif Anae  
dr.rana\_afif@yahoo.com

<sup>1</sup> Department of Materials Engineering, University of Technology, Baghdad, Iraq

<sup>2</sup> Ministry of Industry and Minerals, Commission for Research and Industrial Development, Baghdad, Iraq

<sup>3</sup> Department of Biomedical Sciences, University of Illinois at Chicago, Chicago, USA

<sup>4</sup> Department of Planning and Follow-Up, Ministry of Agriculture, Baghdad, Iraq

14.5 cm, while the diameter of target electrode was 7.5 cm and the distance between them was 3.5 cm.

The gas source-flow controller system is responsible for supplying the feedstock at the desired flow rate and gas pressure to the plasma chamber. It consists of dual-stage regulators, tubing, and fittings for the gas storage cylinders

(Argon). Dual-stage needle valve regulated the flow pressure to the plasma chamber.

The vacuum system consists of a turbo pump (Variant, V-1000HT) assisted by a hydraulic rotary pump (60 m<sup>3</sup>/h, Balzer). The installation of penning (Edward CP25-K with controller 1102) and pirani gauges (LH-Thermovac with Combitron CM350) in the plasma chamber was required

**Fig. 1** SEM/EDS of Nb<sub>2</sub>O<sub>5</sub>-Ni composite coatings with different percents. **a** 0 wt%, **b** 12 wt%, **c** 15 wt%, and **d** 30 wt%

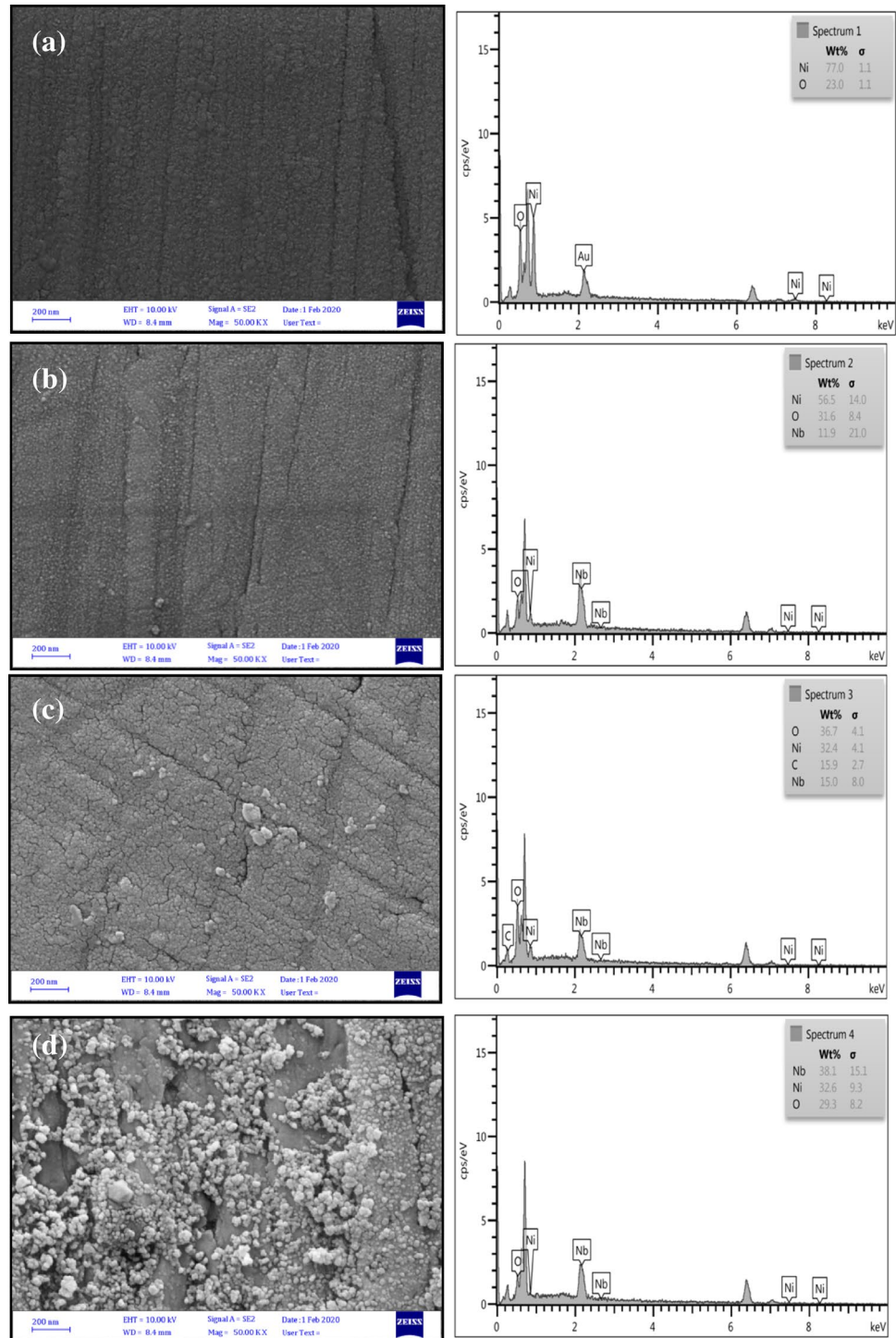
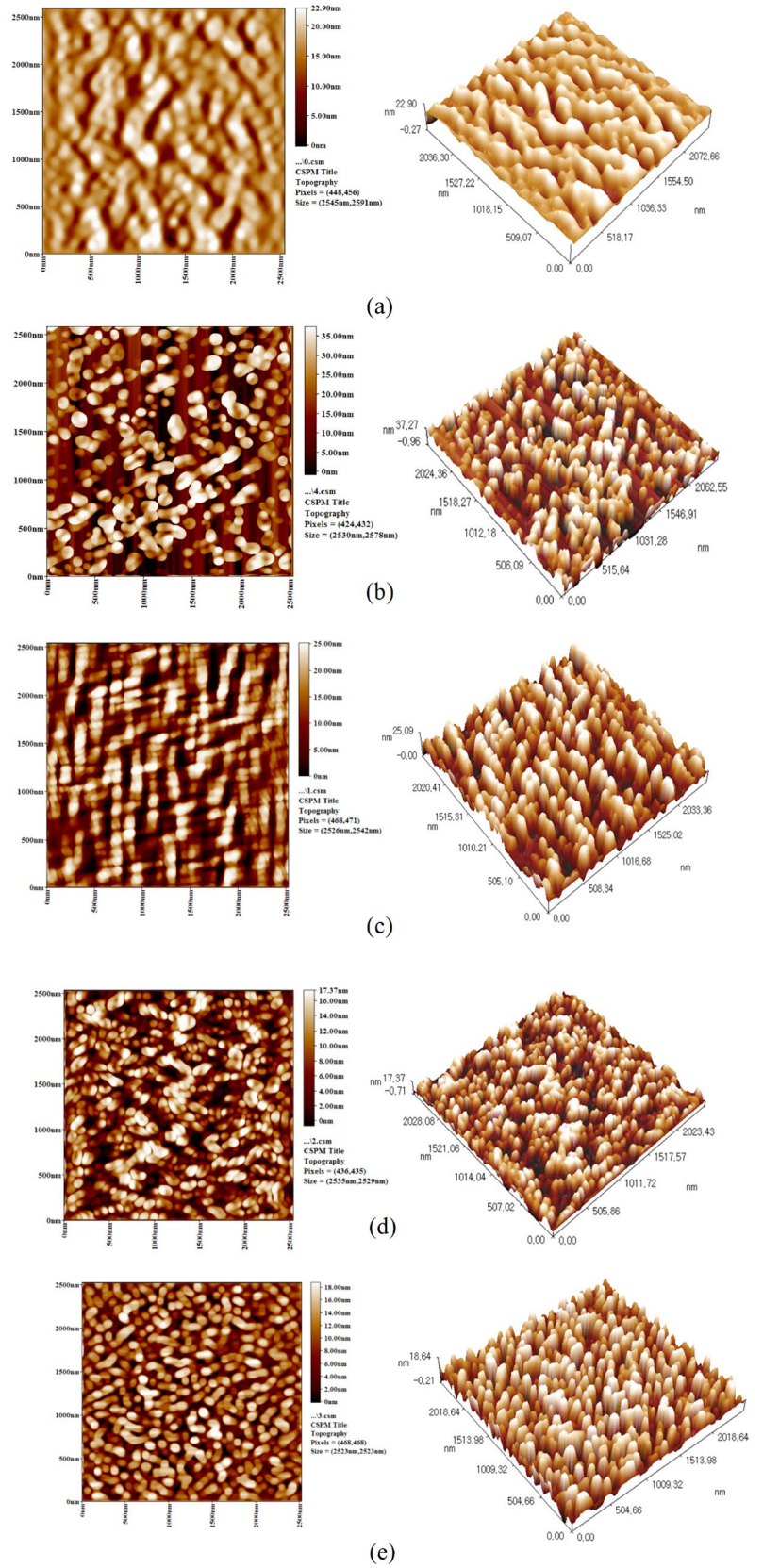


**Fig. 2** AFM images of uncoated steel (a) and Nb<sub>2</sub>O<sub>5</sub>-Ni composite coatings with different percents: **b** 0 wt%, **c** 12 wt%, **d** 15 wt%, and **e** 30 wt%





to monitor the actual pressure and the partial pressure of the discharge gases.

## 2.2 Characterization Methods

The morphologies and chemical compositions of the obtained coating were analyzed using scanning electron microscope (SEM) and its configured energy-dispersive spectrometer (EDS). This test was performed at University of Sanjaya Sheriff Tehran-Iran. The phases were analyzed by X-ray diffraction (XRD), type (Angstrom Advanced Inc model ADX 2700) at Ministry of Science and Technology, Iraq.

The coating roughness was measured using an image analysis from AFM (Model AA3000 Scanning Probe Microscope), at College of Science – University of Baghdad.

The electrochemical test was conducted using WINKINK MLab 200 Potentiostat/Galvanostat from Bank Company at 303 K. The classical three-electrode configuration was composed of platinum rod, saturated calomel electrode (SCE), and steel sample, which were used as the counter electrode, reference electrode, and working electrode, respectively. The working electrode with an area of 1 cm<sup>2</sup> was immersed into the solution for 30 min to attain the stable state of open circuit potential (OCP); the potentiodynamic polarization test was conducted with scanning rate of 10 mV/s.

## 2.3 Microhardness and Thickness

Microhardness values were calculated for coated specimens with load of 9.8 g for 15 s. The average readings were taken for three measurements. Optical method for determining film thickness is commonly used because it refers to both opaque and transparent film and typically yields high-precision thickness value. These tests were performed at the Department of Material Engineering-University of Technology, Iraq.

## 3 Results and Discussion

### 3.1 Morphological Studies

Figure 1 shows the morphological structure of Nb<sub>2</sub>O<sub>5</sub>-Ni composite coatings 0, 12, 15, and 30 wt% of total weight of target, from this Figure can be seen crystallite particles growth distributed on the steel surface within nickel layer. Also, it is clearly showing a perfect incorporation of Nb<sub>2</sub>O<sub>5</sub> within the nickel-rich region. The incorporation of Nb<sub>2</sub>O<sub>5</sub>

particles increased with increasing wt% of Nb<sub>2</sub>O<sub>5</sub> addition due to microstructural bonding and increasing nucleation process in Ni metal as carrier for Nb<sub>2</sub>O<sub>5</sub>.

EDS pattern of deposited Nb<sub>2</sub>O<sub>5</sub>-Ni layers shows combined elemental composition of the deposited composite coating with indication of Ni, Nb, and O present as major components.

Figure 2 shows the AFM images. These images indicate a smooth surface for uncoated surface with very small roughness equal to (2.97 nm) due to atmospheric corrosion with random distribution of particles with highest average diameter (148.06 nm). Ni-coated surface shows some summits and valleys due to deposition of Ni particles and nickel oxide with roughness average (9.52 nm) and more ordered distribution of particles with average diameters equal to (81.14).

The Nb<sub>2</sub>O<sub>5</sub>-Ni composites-coated surfaces gave smoother surface and the smoothness increases with increasing the weight percent of Nb<sub>2</sub>O<sub>5</sub> in composite as shown in Table 1. The decrease in surface roughness can be attributed to the Nb<sub>2</sub>O<sub>5</sub>-incorporated Ni film which enhanced grain growth to obtain a larger particle size as shown in Fig. 3.

### 3.2 Microhardness and Coating Thickness

The microhardness measurement was done for coated specimens and the results are shown in Fig. 4. These data show the higher hardness for Ni-coated surface (155 HV) compared with uncoated surface (132 H.V). Adding Nb<sub>2</sub>O<sub>5</sub> with 12 and 15 wt% to Ni coating decreased the hardness to (139) and (148), respectively, because of the presence of some pores within the coating. While adding the higher weight percent (30 wt%) of Nb<sub>2</sub>O<sub>5</sub> led to increasing the hardness to (164 HV) due to filling of the pores within Ni layer.

The incorporation of Nb<sub>2</sub>O<sub>5</sub> within Ni coating led to slight increases in thickness of coating by ≈ 1 μm because of filling of the gaps as shown in Fig. 4.

### 3.3 Corrosion Characteristics

The results of the corrosion progression in 3.5 wt% NaCl at 303 K from the linear potentiodynamic polarization

**Table 1** AFM data for uncoated and coated samples

Material coating	Roughness average (nm)	Average diameter of surface (nm)
Uncoated steel	2.97	148.06
Ni coating	9.52	81.14
12%Nb <sub>2</sub> O <sub>5</sub> -Ni coating	6.27	97.72
15%Nb <sub>2</sub> O <sub>5</sub> -Ni coating	4.72	87.00
30%Nb <sub>2</sub> O <sub>5</sub> -Ni coating	4.53	74.44

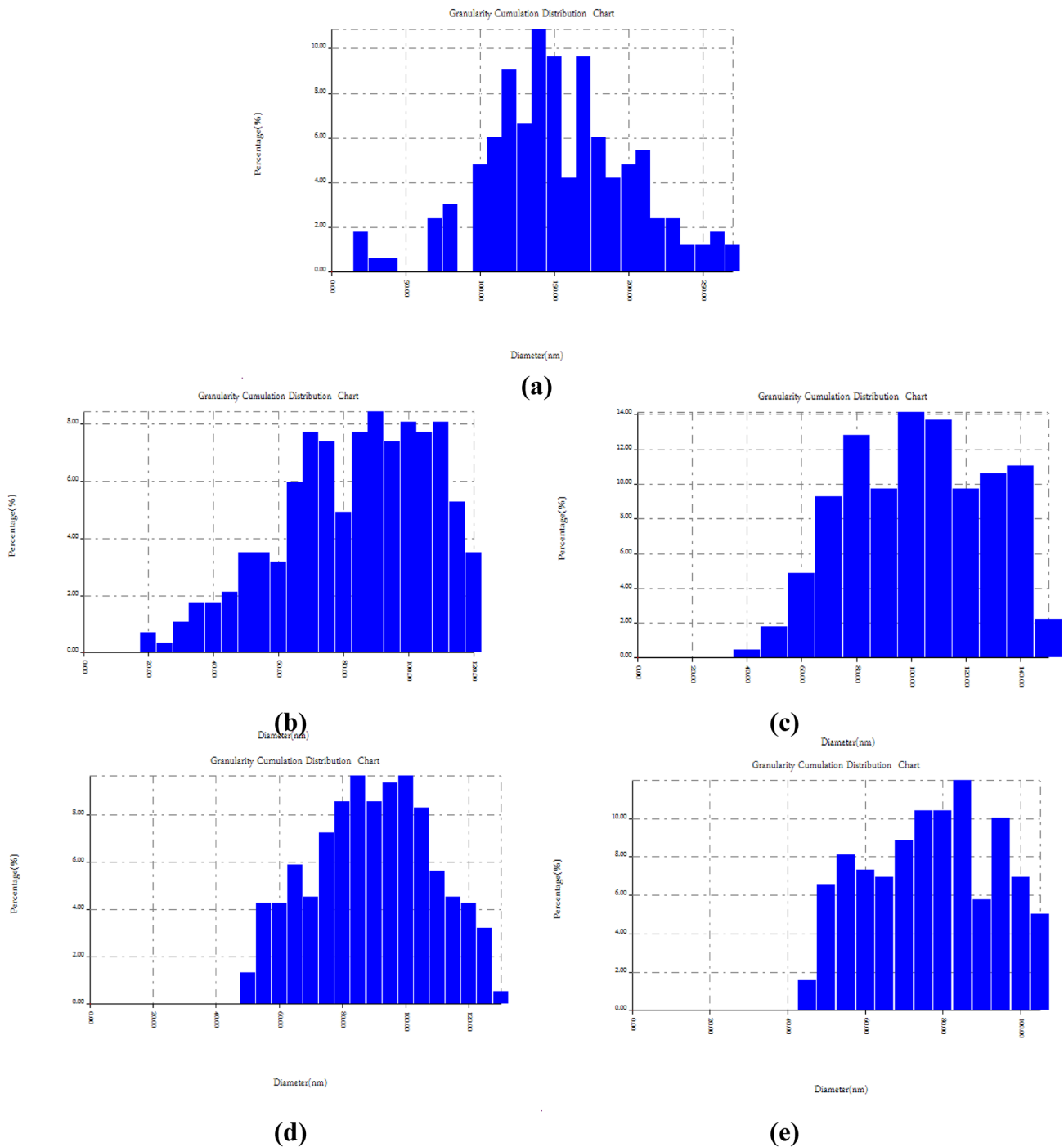


**Fig. 3** Distribution chart of particles of uncoated steel **(a)** and Nb<sub>2</sub>O<sub>5</sub>-Ni composite coatings with different percents: **b** 0 wt%, **c** 12 wt%, **d** 15 wt%, and **e** 30 wt%

study are shown in Fig. 5 and Table 2. The Tafel data were extrapolated to obtain  $E_{\text{corr}}$ ,  $i_{\text{corr}}$ , and Tafel slopes. From the polarization curves of the Nb<sub>2</sub>O<sub>5</sub>-Ni composite coatings on carbon steel, it can be seen that corrosion potential ( $E_{\text{corr}}$ ) was shifted toward more noble value due to attaining passivity. The corrosion current density ( $i_{\text{corr}}$ )

was decreased with increasing wt% of Nb<sub>2</sub>O<sub>5</sub> in Ni coating confirming the role of protection of applied coatings. Tafel slopes ( $b_c$  &  $b_a$ ) decreased referring to reducing the reactions at cathodic and anodic sites.

Polarization resistance ( $R_p$ ) can be calculated by the following formula [11]:

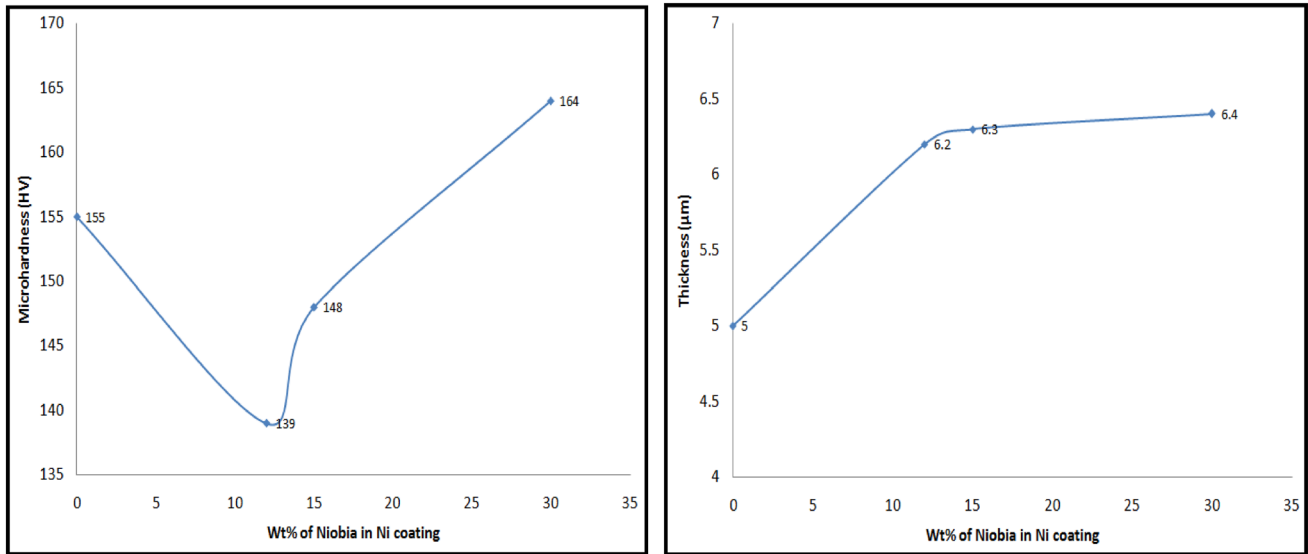


Fig. 4 Microhardness and thickness of Nb<sub>2</sub>O<sub>5</sub>-Ni-coated specimens

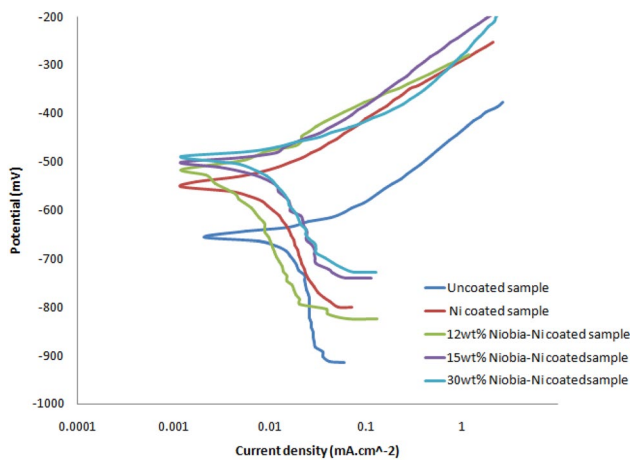


Fig. 5 Tafel plots of uncoated and coated specimens at 303 K

Table 2 Corrosion data of uncoated and coated steel at 303 K

Coating type	$-E_{corr}$ mV	$i_{corr}$ $\mu A\ cm^{-2}$	$-b_c$ $mV\ dec^{-1}$	$+b_a$
Uncoated steel	656	15.49	571.5	89.8
Ni coating	552	5.72	177.3	80.2
12%Nb <sub>2</sub> O <sub>5</sub> -Ni coating	517	4.51	184.2	73.4
15%Nb <sub>2</sub> O <sub>5</sub> -Ni coating	509	3.67	154.3	89.5
30%Nb <sub>2</sub> O <sub>5</sub> -Ni coating	490	2.97	151.8	71.5

$$R_p = \frac{(b_c \times b_a)}{2.3 \times i_{corr}(b_c + b_a)} \tag{1}$$

The data of  $R_p$  as listed in Table 3 indicate that the polarization resistance increased with increasing Nb<sub>2</sub>O<sub>5</sub> percent in Ni coating because of filling of the pores within the Ni layer.

Other parameters can be calculated from corrosion data such as protection efficiency (PE%) from corrosion current density of coated sample ( $i_{corr, coated}$ ) and corrosion current density of uncoated sample ( $i_{corr, uncoated}$ ) as follows [12]:

$$PE\% = \left[ 1 - \frac{i_{corr, coated}}{i_{corr, uncoated}} \right] \times 100 \tag{2}$$

The protection efficiency increases with increasing wt% of Nb<sub>2</sub>O<sub>5</sub> in coating composite to get the best efficiency equal to 80.826% for 30% Nb<sub>2</sub>O<sub>5</sub>-Ni mixture. The porosity percentage (PP%) can be calculated from the polarization

Table 3 Protection properties of uncoated and coated steel at 303 K

Coating type	$R_p \times 10^3$ $\Omega\ cm^2$	PE%	PP%
Uncoated steel	2.178	–	–
Ni coating	4.197	63.072	3.605
12%Nb <sub>2</sub> O <sub>5</sub> -Ni coating	5.060	70.884	1.219
15%Nb <sub>2</sub> O <sub>5</sub> -Ni coating	6.711	76.307	0.748
30%Nb <sub>2</sub> O <sub>5</sub> -Ni coating	7.115	80.826	0.433

resistance of uncoated ( $R_{p,uncoated}$ ) and coated ( $R_{p,coated}$ ) sample using the following equation [13]:

$$PP\% = \frac{R_{p,uncoated}}{R_{p,coated}} 10^{\frac{-\Delta E_{corr}}{b_a}} \times 100. \quad (3)$$

The porosity percentage increases with increasing wt% of Nb<sub>2</sub>O<sub>5</sub> in nickel layer to get the best value of 0.433% for 30% Nb<sub>2</sub>O<sub>5</sub>-Ni composite coating due to incorporation of Nb<sub>2</sub>O<sub>5</sub> with Ni layer.

## 4 Conclusions

Nb<sub>2</sub>O<sub>5</sub>-Ni composite coatings were successfully fabricated using DC sputtering.

The structural properties indicate the presence of Nb<sub>2</sub>O<sub>5</sub> within Ni coating by SEM/EDS and AFM.

Good corrosion resistance was attained for all deposited coatings as against the as-received specimen.

The significant performance improvement in the protection efficiency and porosity percentage was found as a result of physical barriers produced by Nb<sub>2</sub>O<sub>5</sub> particles by filling of the pores within the Ni layer.

## References

- Huang Y, Zhang Y, Hu X (2003) Structural morphological and electrochromic properties of Nb<sub>2</sub>O<sub>5</sub> films deposited by reactive sputtering. *Solar Energy Mater Solar Cells* 77:155–162
- Serényi M, Lohner T, Petrik P, Zolnai Z, Horváth ZE, Khanh NQ (2008) Characterization of sputtered and annealed niobium oxide films using spectroscopic ellipsometry, Rutherford backscattering

spectrometry and X-ray diffraction. *Mater Sci Thin Solid Films* 516:8096–8100

- Olivares-Navarrete R, Olaya JJ, Ramírez C, Rodil SE (2011) Biocompatibility of niobium coatings. *Coatings* 1:72–87
- Rojas PN, Rodil SE (2012) Corrosion behaviour of amorphous niobium oxide coatings. *Int J ElectrochemSci* 7:1443–1458
- Rodrigues PRP, Terada M, Junior ORA, Lopes AC, Costa I, Banczek EP (2014) Niobium pentoxide coating replacing zinc phosphate coating. *RevistaMatéria* 19(02):105–116
- Chen H, Wang Q, Dong H, Xi L, Lin X, Pan F, Ma Z (2015) Electroless plating of Ni-P-W coatings containing scattered Nb<sub>2</sub>O<sub>5</sub> on sintered NdFeB substrate. *Mater Res* 18(5):1089–1096
- Joshi P, Gesawat AA, Singh K (2015) Development and characterization of Ti-Nb-N coatings on stainless steel using reactive DC magnetron sputtering. *ChemSci Rev Lett* 4(16):1059–1068
- Mohan Reddy R, Praveen BM, Praveen Kumar CM (2017) Corrosion behavior and characterization of Ni-Nb<sub>2</sub>O<sub>5</sub> composites prepared by pulse electro deposition. *Surf EngApplElectrochem* 53(2):179–185
- Oluyori T, Olorunniwo OE, Fayomi OSI, Atanda PO, Popola API (2017) Performance evaluation effect of Nb<sub>2</sub>O<sub>5</sub> particulate on the microstructural, wear and anti-corrosion resistance of Zn-Nb<sub>2</sub>O<sub>5</sub> coatings on mild steel for marine application. *J Bio TriboCorros* 3(51):2–6
- Shi K, Zhang Y, Zhang J, Xie Z (2019) Electrochemical properties of niobium coating for biomedical application. *Coatings* 9:546
- Yaqo EA, Anaee RA, Abdulmajeed MH, Tomi IHR, Kadhim MM (2019) Aminotriazole derivative as anti-corrosion material for Iraqi kerosene tanks: electrochemical, computational and the surface study. *ChemistrySelect* 4:9883–9892
- Anaee RA, Abd Al-Majeed MH, Naser SA, Kathem MM, Ahmed OA (2019) Antibacterial inhibitor as an expired metoclopramide in 0.5M phosphoric acid. *Al-Khwarizmi Eng J* 15(1):71–81
- Anaee RA (2015) Properties of functionally graded coating of Al<sub>2</sub>O<sub>3</sub>/ZrO<sub>2</sub>/HAP on SS 316L. *Intl J SciEng Res* 6(5):953–957

**Publisher's Note** Springer Nature remains neutral with regard to jurisdictional claims in published maps and institutional affiliations.